

Cost benefit analysis of supercritical CO₂ cycles in next-generation solar thermal power plants

Lukas Heller^a, Stefan Glos^b, Reiner Buck^a

^a German Aerospace Center (DLR), Institute of Solar Research, Stuttgart, Germany

^b Siemens Energy, Mülheim an der Ruhr, Germany

ARTICLE INFO

Keywords:

Supercritical CO₂
CSP
Techno-economic
Particle technology

ABSTRACT

Proposed future solar thermal power plant technologies commonly feature high-temperature supercritical CO₂ (sCO₂) power cycles due to predicted high thermal efficiencies and low capital costs. However, as the technology also poses significant challenges, a detailed techno-economic comparison is needed to assess potential benefits over state-of-the-art steam cycles. In this study, detailed thermodynamic models of six sCO₂ cycles and a reference steam cycle as well as cost correlations for their main components were developed. The models were used for hourly simulations to derive the plants' annual energy yields and levelized cost of electricity. Results show that the levelized cost of any sCO₂ process is at least 9% higher than that of the reference system. Although there is considerable uncertainty in some of the components' cost models, even lowering the costs of most sCO₂-specific components by 50% did not lead to cost parity. This indicates that the development of next-generation solar thermal plants should include modern steam power cycles.

1. Introduction

The use of supercritical carbon dioxide (sCO₂) as the working fluid in power cycles has received a great amount of interest in recent years. Applications have been proposed, among others, for nuclear, coal, concentrating solar power (CSP), geothermal or waste heat as the energy source. Commonly stated advantages of sCO₂ over state-of-the-art steam power cycles are higher thermal efficiencies, lower installation costs, smaller footprints and faster response times [1].

However, the technology also poses significant challenges, mainly in the fields of materials (under very high temperatures and pressures), turbomachinery (closeness to the critical point) and heat exchanger development as well as plant operation. In order to compete with the well-established state of the art in utility-scale power generation, i.e. water/steam, the aforementioned benefits of sCO₂ cycles have to overcompensate the costs associated with overcoming these challenges. For commercial projects (with technology-agnostic boundary conditions) this means, generally speaking, that the cost of generated electricity needs to be lower.

Whether the implementation of an sCO₂ power block leads to lower cost of electricity for a specific application depends on technology-dependent parameters, most importantly the temperature range in which thermal energy is provided to the cycle. Closed cycle heat

sources (like nuclear, geothermal and CSP) are particularly advantageous for efficient sCO₂ cycles, due to the latter's high rate of recuperation [2]. Next-generation CSP plants, which are predicted to be commercially available before the year 2030 [3], appear especially suitable to high-efficiency cycles, as they are designed to reach temperatures upwards of 700 °C. Furthermore, the use of CSP as a heat source in combination with cost-effective thermal storage offers advantages compared to photovoltaic systems with batteries, especially for long storage durations [4].

A large number of studies that show the great thermodynamic potential of sCO₂ cycles for CSP systems have been conducted in the last decade (see [5]). Thermal efficiencies above 50% are commonly stated [6], however these are only reached with a combination of very large internal heat exchangers (recuperators), high turbine inlet temperatures and several compression stages (e.g. recompression). All of these features increase the cost of the power block considerably. Furthermore, highly efficient sCO₂ cycles also tend to have a small temperature spread in the primary heat exchanger, which negatively influences the solar and storage subsystems of a plant [7]. It is, hence, necessary to model a complete plant in order to assess its economic viability [8].

There are a few studies, in which the techno-economic performance of CSP plants featuring sCO₂ cycles has been quantified. Ho et al. [9]

* Corresponding author.

E-mail address: Lukas.Heller@dlr.de (L. Heller).

Nomenclature

Variables

A	Area (m^2)
C	Cost (USD)
$LCOE$	Levelized cost of electricity ($\text{USD}/(\text{kW}_e \text{ h})$)
p	Pressure (Pa)
TIT	Turbine inlet temperature (K)
TTD	Terminal temperature difference (K)
U	Conductance ($\text{W}/(\text{m}^2\text{K})$)
η	Efficiency (%)

Subscripts

e	Electrical
FLE	Full load-equivalent
m	Mechanical
t	Thermal

Abbreviations

BoP	Balance of plant
CSP	Concentrating solar power
HTM	Heat transfer medium
LCOE	Levelized cost of electricity
PB	Power block
PHX	Primary heat exchanger
PV	Photovoltaics
sCO ₂	Supercritical carbon dioxide
TES	Thermal energy storage
TIT	Turbine inlet temperature

calculated the installation cost of power blocks and complete plant costs for molten salt systems featuring different sCO₂ power cycles. For simple recuperated and recompression cycles, both reaching a thermal efficiency of 46%, they state a very similar cost for each of the power blocks of approximately 900 USD/kW_e, and for the total plant below 4000 USD/kW_e. The latter value is lower than for comparable CSP plants with steam cycle.

Merchán et al. [8] also compared installation costs for generic CSP plants with sCO₂ cycles of different layouts and optimized parameters. They found that partial cooling cycles had lower costs than simple recuperated and recompression cycles in almost all cases, however, the difference was rather small at less than 5%. The results were not compared to steam cycles.

Cheang et al. [10] also used the total plant cost as a metric for a direct comparison between molten salt CSP plants with sCO₂ cycles and with state-of-the-art superheated and supercritical steam cycles. They designed the subsystems of these plants for different ambient temperatures and concluded that all of the sCO₂ power blocks suffer from lower efficiencies and higher total costs than the steam configurations. The main cost drivers for the power block were found to be fluid compression, recuperation and cooling. According to their models, all other subsystems of the plant furthermore contribute to increased total costs due to a considerably lower power cycle efficiency. The thermal energy storage (TES) system costs increased further due to the smaller temperature spread between hot and cold salt tanks. In conclusion, the authors recommend research for CSP plants to focus on applications with existing steam technology as power cycles.

Crespi et al. [11] calculated the total plant cost for ten different sCO₂ cycle designs and considered probabilistic cost correlations. They modeled a system using next-generation high-temperature molten salt

allowing for a very high working fluid temperature (750 °C) and, therefore, reaching elevated thermal efficiencies between 45% and 53%. Among those layouts relevant for indirectly heated applications at typical CSP locations, they found the partial cooling cycle to have the highest probability of reaching the lowest overnight cost, followed by a simple recuperated and a precompression layout. They further state that these three layouts likely have lower cost than values given for state-of-the-art CSP plants.

In a follow-up study, Crespi et al. [12] simulated the annual yield of the most promising of the above-mentioned systems (partial cooling cycle), one Allam cycle layout (which is directly fired) and one featuring a standard steam cycle. This enabled the authors to then compare their levelized cost of electricity (LCOE) and, through a dispatch and price scheme, different projects' net present value. In terms of these two financial performance indicators, the final results of all three systems are very close and their confidence intervals mostly overlap, meaning that no clear benefit could be identified for any of them. This highlights the importance of comparing such indicators for results generated with comparable models and close to identical boundary conditions.

Neises and Turchi [13] also compared the annual performance of molten salt CSP plants employing variations of different sCO₂ cycles. However, they considered a more conventional molten salt composition, allowing for working fluid temperatures of up to 630 °C. Comparing the cycles' LCOE, they concluded that while recompression cycles reach the highest thermal efficiency, partial cooling cycles achieve lower LCOE due to their larger temperature spread (causing lower pumping parasitics and TES system costs). Furthermore, the simple recuperated cycle has a considerably lower installation cost because of its less complex layout which leads to comparable LCOE to the recompression cycle configurations despite the lower thermal efficiency. Neises and Turchi did not compare the results to those of a steam cycle plant.

Guccione and Guedez [14] evaluated several sCO₂ and steam cycles in combination with CSP, photovoltaics (PV), electric heaters and molten salt TES systems techno-economically. They found adding PV particularly beneficial in small systems at locations with a low share of direct normal irradiance. Replacing the steam power block with an sCO₂ cycle was found to bring further cost reductions.

CSP plants generally employ dry cooling technology due to their location in mostly hot and arid areas. This, however, prevents lowering the sCO₂ temperature in the cooler below its critical point during most of the year [15]. Manzolini et al. [16] addressed the potential of improvements to plant performance by blending sCO₂ with additives in order to increase its critical temperature. In a comparison of three cycles, the LCOE of a plant featuring an sCO₂-based mixture was only marginally lower than that of the ones using pure sCO₂ or steam. Rodríguez-deArriba et al. [17] calculated maximum threshold costs for the sCO₂ blend power cycle of two different CSP plant technologies. They found in the more promising case, the power block costs (at a turbine inlet temperature of 700 °C) can be up to 20% higher than the reference steam system to achieve the defined cost goals. Several detailed aspects of such blends in CSP plants have been investigated, e.g., heat transfer characteristics [18] and cooling system operation [19].

An alternative heat transfer medium (HTM) to molten salts are solid particles. Due to their low cost, high-temperature stability and lack of freezing issues, they are seen as the most likely replacement for state-of-the-art molten salt in future CSP plants [3]. These advantages also make them particularly well-suited for coupling with sCO₂ power cycles: The high upper temperature limit (>1000 °C) enables high conversion efficiencies and the low material cost (potentially combined with a large temperature spread between hot and cold tanks) is a prerequisite for a cost-effective direct TES system. The authors of this present study compared the techno-economics of sCO₂ cycles in state-of-the-art molten salt tower systems to next-generation particle systems [20]. The results indicated a strong preference for particle technology configurations mainly due to lower TES system costs, caused by a much higher temperature spread between hot and cold tank.

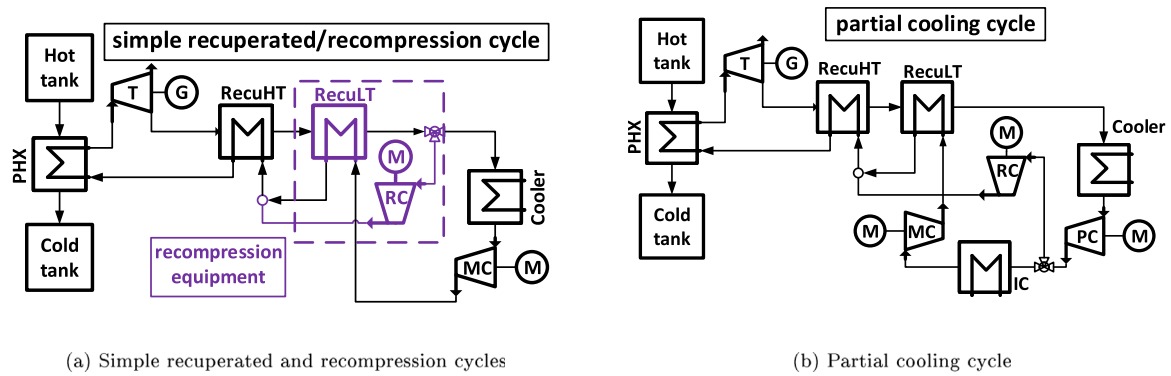


Fig. 1. Schematics of $s\text{CO}_2$ cycles; components drawn in purple color are only implemented in the recompression cycle; PHX: primary heat exchanger; T: turbine, RecuHT: high-temperature recuperator; RecuLT: low-temperature recuperator; MC: main compressor; RC: recompressor; PC: precompressor; IC: intercooler; M: motor; G: generator.

Table 1
Definition of modeled $s\text{CO}_2$ cycles (TTD: terminal temperature difference).

Parameter	Unit	c01_550	c01_650	c05_550	c05_650	c10_550	c10_650
Cycle	[-]	simple recuperated		recompression		partial cooling	
TIT	[°C]	550	650	550	650	550	650
Turbine inlet pressure	[bar _a]		260		260		260
Main compressor inlet pressure	[bar _a]		75		75		80
Precompressor inlet pressure	[bar _a]	-		-			55
TTD _{RecuHT}	[K]	5	5	25	15		5
(UA) _{maincooler}	[MW/K]	14.0	10.5	17.5	14.0	10.5	7.0
(UA) _{intercooler}	[MW/K]	-		-			10.5
Recompression fraction	[%]	-		30	35	45	40
$\eta_{PB,net}$	[%]	37.0	41.0	38.9	44.4	40.4	44.1

Subsequently, Heller et al. [21] modeled numerous particle systems for selecting the most suitable $s\text{CO}_2$ cycle layouts and their parameters for CSP applications on the basis of a preliminary techno-economic evaluation. Simulation results confirmed those found in some of the previously mentioned studies, namely that (a) simple recuperated cycles can have considerably lower cost than more complex layouts, (b) partial cooling cycles are comparable or preferable to recompression cycles and (c) it is by no means a given that replacing a modern steam cycle with an $s\text{CO}_2$ cycle benefits overall system costs. In some aspects, the results indicated an even stronger preference for cost-effective low-efficiency $s\text{CO}_2$ cycles (at more conventional fluid parameters) than previously published. However, the conducted studies were solely based on design-point simulations of the cycles' and plants' performance and on estimated conversion factors to annual yield. Furthermore, the solar field size and TES capacity were not optimized. Therefore, economic optima for the whole plant might have been missed, potentially leading to differences in rankings among $s\text{CO}_2$ cycles and in the comparison to steam systems.

Building on the findings of these works, this present study aims at giving a robust answer to the question whether next-generation CSP plants will benefit from incorporating pure $s\text{CO}_2$ cycles instead of commercially available steam power cycles. Necessary steps to this end, which are addressed in the following, are: The definition of layouts to be compared as well as their parameters and boundary conditions, the detailed thermodynamic design and off-design modeling of these layouts for annual energy yield calculations, the selection of realistic cost correlations at the necessary level of detail, the critical comparison of the variants' results, sensitivity analyses and a conclusion on the findings taken into account the models' inherent limitations.

2. Plant configurations

The techno-economic performance of $s\text{CO}_2$ power plants depends on numerous factors. In this section, the boundary conditions common to all modeled plants, the compared power cycles ($s\text{CO}_2$ as well as steam) and the particle CSP systems are described.

2.1. Boundary conditions

Utility-scale CSP plants with a nominal net power block rating of 112 MW_e are analyzed. A location in the Northern Cape Province of South Africa was chosen due to a very high annual solar radiation (see Appendix A). As is common for favorable CSP plant locations, dry cooling has to be employed for water scarcity and ambient temperatures can reach high values during the day. This results in more challenging off-design plant control, lower thermal efficiencies and higher cost for cooling equipment compared with typical locations of fossil-fired plants. The design point ambient temperature is set to 19 °C, the annual average of the site. No specific demand curve is defined so that electricity can be fed into the grid whenever sufficient thermal energy is available.

2.2. $s\text{CO}_2$ cycles and components

In a previous study by the authors [21], ten different $s\text{CO}_2$ cycle layouts were modeled based on simple recuperated, recompression and partial cooling cycles. For several thousand variants of these layouts (defined by cycle parameters like, e.g., turbine inlet temperature, cycle minimum and maximum pressure, rating of heat exchangers and recompression fraction), the design point performance was determined. Furthermore, an annual efficiency of the solar field and a relative design point-to-annual power cycle efficiency conversion factor were estimated in order to calculate each variant's annual electric yield. Adding cost models on the subsystem level and, in case of the power block, on the component level enabled the techno-economic comparison of all variants.

The results of that study indicate that adding reheating and intercooling to the basic cycles does not improve their economic performance. The same is true for increasing the turbine inlet temperature (TIT) above 550 °C. For the detailed simulation in the present study, a basic layout of each of the three $s\text{CO}_2$ cycles, as depicted in Fig. 1, was modeled at two TIT levels (550 °C and 650 °C). The former was chosen because it generally resulted in the lowest LCOE in the pre-study and

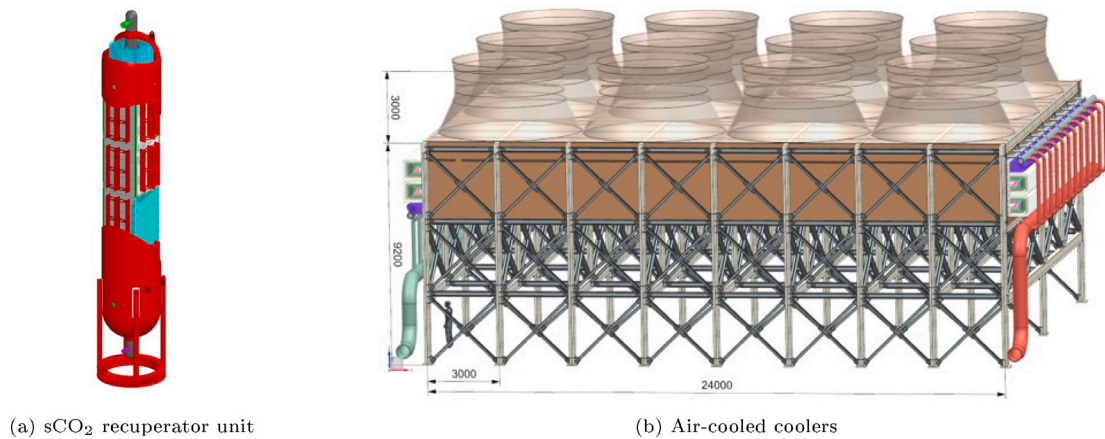


Fig. 2. 3D visualization of $s\text{CO}_2$ HX designs (shown distances are in millimeter).

the latter for including higher efficiency cycles favored in many other studies. For each of the resulting six configurations, those parameters were chosen that resulted in the lowest LCOE in the pre-study or in slightly higher values ($< +1.5\%$) while allowing the use of identical components for several variants. The parameters are presented in Table 1, temperature–entropy diagrams in Appendix B and state points in Appendix C.

Siemens Energy AG designed turbines, compressors, recuperators and air coolers based on these parameters. The $s\text{CO}_2$ turbine designs are derived from high-pressure steam turbines. For variants with a TIT of 650°C , high-performance alloys have to be used. For all compressors, multi-stage barrel-type units with a single shaft are foreseen.

As recuperators, header-type shell-in-tube heat exchangers were chosen (see Fig. 2, left). Due to size limitations, some cycle variants feature two units in parallel per recuperator, leading to additional pressure losses in manifolds. In literature, compact heat exchangers are commonly proposed as a more space- and cost-effective technology for $s\text{CO}_2$ recuperators. However, there is large uncertainty in terms of cost associated with this technology which is yet unproven at scale. Furthermore, compact heat exchangers can currently only be manufactured in small geometries, necessitating a large number of units to be installed in parallel to achieve the needed heat transfer surface area for a utility-scale power block. This is expected to cause high pressure drops to which $s\text{CO}_2$ cycles' performance is sensitive. For these reasons, the established shell-in-tube technology was chosen instead.

The high fluid pressure of up to 80 bar_a in all coolers presents a challenge. The chosen design is based on air-cooled steam condensers, however with much thicker tubes, similar to heat recovery steam generators (depicted in Fig. 2, right). The cooler size is limited by available tube length (approximately 24 m), so that all modeled configurations require at least three such units.

2.3. Reference steam cycle

To assess potential cost benefits of employing a new technology, a reference needs to be defined. Subcritical steam cycles are installed in practically all existing CSP plants and, therefore, comprise the state of the art. In plants using molten salt as the HTM, these cycles are commonly designed for TITs above 540°C but below 560°C due to the HTM's operating limits. They, furthermore, feature a re-heat stage as well as several steam extraction points to boost their efficiency. The reference system's power block was designed by Siemens Energy and is based on such a state-of-the-art cycle (single reheat stage; TIT of 550°C ; live/re-heat steam pressure: $> 160\text{ bar}/> 30\text{ bar}$) and yields a net power block efficiency ($\eta_{\text{PB,net}}$, net electric output of power block divided by thermal input to the primary heat exchanger) of 43.7% at the design point. This is a rather high value for a subcritical steam CSP

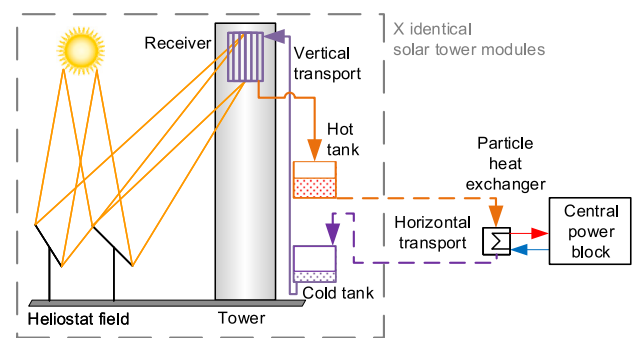


Fig. 3. Schematic of the solar particle loop [21].

cycle, however, comparable values have been reported for similar high re-heat pressure cycles [22] and are further caused by the low ambient design-point temperature of 19°C .

Higher TITs and efficiencies could be reached in a steam cycle when heated by particle technology. However, Heller et al. [21] found slightly higher LCOE for a high-performance steam cycle, which would still require considerable development efforts, compared with the above-mentioned state of the art. Hence, only the commercially available steam process was modeled as the reference system in this study.

2.4. Particle CSP system

The plants' solar particle loop, including the solar field, HTM, TES and PHX (primary heat exchanger) subsystems, is depicted in Fig. 3. The plant concept, which is described in more detail by Buck [23] and Heller et al. [24], has been designed around the CentRec[®] centrifugal particle receiver technology [25]. Demonstrators of this receiver technology have been tested at particle outlet temperatures of up to 965°C [26]. At such temperatures, thermal efficiencies above 90% have been predicted for commercial designs [23].

Thermal losses in CentRec[®] receivers are minimized by a cavity design, which, however, causes excessive optical losses (spillage) in utility-scale single-tower heliostat fields [24]. Hence, the concept foresees a multi-tower setup in which a single receiver is located on top of each one of a multitude of individual towers, featuring a dedicated heliostat field. In the current study, comparatively large receiver units with a rating of 96 MW_t each have been assumed. The particles are stored in decentralized hot and cold tanks integrated into the structure of each tower and are transported in insulated containers to and from a central PHX and power block. The number of identical towers and

Table 2

Design-point parameters of sCO₂ cycle components (Δp : pressure drop; η : efficiency; m: mechanical; e: electric; t: thermal; †: relative to design inlet pressure; *: at 1500 kg/s).

Parameter	Value
$\Delta p_{\text{recuperator}}$ low-pressure side	2.0% †
$\Delta p_{\text{recuperator}}$ high-pressure side	3.0% †
Δp_{PHX}	2.0% †
$\Delta p_{\text{cooler/pre-cooler}}$	0.6% †
$\Delta p_{\text{cooler/pre-cooler,airside}}$	5.0 mbar*
$\eta_{\text{turbine,isentropic}}$	91.5%
$\eta_{\text{compressor,isentropic}}$	85.9%
$\eta_{\text{fan,isentropic}}$	87.3%
$\eta_{\text{turbine,m}} \times \eta_{\text{generator,e+m}}$	98.5%
$\eta_{\text{motor,e+m}} \times \eta_{\text{compressor/fan,m}}$	95.8%
$\eta_{\text{PHX,t}}$	99.0%

the TES capacity can be varied in order to influence a plant's capacity factor and optimize it for minimum LCOE. This is further explained in Section 3.2. The defining parameters of the particle CSP system are given in an extensive databook in Appendix A.

3. Modeling and simulations

In order to compare the six chosen sCO₂ cycles with the reference steam case techno-economically, a thermodynamic model of each of them is created. In combination with performance models for the solar particle loop, they are used to calculate the electric yield of a particle CSP plant for every hour of a typical meteorological year. Finally, cost models for all plant subsystems are developed to derive the investment cost and LCOE of each configuration.

3.1. Thermodynamic power cycle models

All seven power cycles are modeled in the power plant simulation software Epsilon[®] Professional 14.03 by STEAG Energy Services GmbH. These models are used for three purposes: (I) The design-point heat input into the PHX is derived to size the TES and parts of the particle transport system. (II) The rating of turbine, generator, compressors, fans, motors and heat exchangers are determined to calculate their investment cost (see Section 3.3). (III) The net electric yield of the power block is simulated for every hour of the year, depending on ambient conditions and available thermal energy. This includes parasitic consumption for the coolers' air fans.

Some general component performance parameters, which were used for all sCO₂ cycle models, are given in Table 2. The values for pressure drops are identical to the ones by Heller et al. [21], some of the component efficiencies have been updated during their detailed design within the present study. In the following, some further detail is given on the modeling of heat exchangers, due to their large impact on cycle performance and cost.

Non-linear changes of fluid properties close to the critical point require that coolers are discretized. In the developed models, each cooler comprises five serial subsections with the identical heat transfer surface area. No significant change in performance was found when increasing the number of units further. Counter-flow heat exchanger elements are implemented into the model, although the actual design is a cross-flow design based on air-cooled steam condensers. A "cross-flow efficiency", $\eta_{\text{cross-flow}} = 95\%$, is added to account for less effective heat transfer:

$$(UA)_{\text{cooler}} = (UA)_{\text{counter-flow}} / \eta_{\text{cross-flow}} \quad (1)$$

Recuperators, on the other hand, are only discretized in a post-processing model in order to determine their total conductance (see Purpose (II) above). For hourly performance simulations, the model could be simplified to a single heat exchanger element for each recuperator without loss of accuracy. PHXs do not need to be discretized as their operating temperatures are far from the critical point of sCO₂.

3.1.1. Off-design modeling

To realistically simulate the annual electric yield of a CSP plant, the off-design performance of the power cycle needs to be modeled. The two main parameters that should be taken into account are the electric load and the ambient temperature. As no demand profile of the grid was defined in the present study, the power block mostly operates at full load or not at all so that part-load operation is only of secondary importance. The ambient temperature, on the other hand, varies greatly in areas suitable for CSP plants. At the chosen location, operation at temperatures between 5 °C and 35 °C should be assured.

Although numerous studies on the off-design operation of sCO₂ cycles have been published in recent years, these mainly focus on adapting load as demanded by grid requirements and not on changes in cycle performance due to ambient conditions (e.g., [27]). In cases in which cycle operation and control under changing cooling conditions was investigated, it was almost always done only for a specific cycle (mostly of the recompression type [28]). As the current study is not aimed at optimizing one or all of the considered power cycles but rather at comparing them to a reference technology, one generic off-design operating concept was defined for all cycles. It follows the following steps in the given order (compare with Fig. 1):

1. The cooling air mass flow is adjusted to achieve the design-point compressor inlet temperature. The maximum air mass flow is equal to 1500 kg/s per unit.
2. The inlet pressure of main compressor and pre-compressor is adjusted to achieve the design-point volumetric flow rates at the compressor inlet. This ensures stable compressor operation in a region of strongly varying fluid properties. The minimum pressure is equal to the respective design-point value, the maximum is set to 100 bar.
3. The recompression fraction is adjusted to achieve the design-point volumetric flow rate into the recompressor.
4. The sCO₂ mass flow is adjusted to achieve the design-point net power block output. The maximum value is equal to the design-point value. This only applies if the ambient temperature is lower than at the design point and, hence, the cooling power is lower. As the effect is rather small, the sCO₂ mass flow is almost always at its design-point value except if the storage charge level is insufficient.
5. The particle mass flow is adjusted to achieve the design-point TIT.

This strategy leads to almost constant compressor and turbine efficiencies. However, lowered pressure ratios and mass flow rates cause lower power output and efficiencies when ambient temperatures exceed the design point. Furthermore, due to the chosen restrictions, the cycles' gross efficiencies do not significantly increase during times of lower ambient temperatures (see Section 4).

The off-design performance of the reference cycle is defined by the condensate pressure as a function of ambient temperature. Turbine stage pressures are calculated according to Stodola's law. The model was validated with off-design data by Siemens energy.

One of the potential advantages of sCO₂ power cycles compared with the state of the art is load flexibility. It is commonly assumed that due to much more compact equipment, start-up times and energy consumption could be reduced significantly (e.g., from 30 min to 10 min for a warm-start [17]). Taking into consideration the very thick housing of sCO₂ turbines and potential stability issues in supercritical turbomachinery [29,30], the difference could be much smaller. Even if the duration of warm-starts could be halved to 15 min and full-load thermal input into the cycle during the period is assumed, the difference in annual electric yield would be less than 1%. Therefore, and due to a lack of detailed information on the start-up procedure, it was decided to neglect the energy demand for the start-up procedure of both technologies.

3.2. Solar particle loop

The solar field and particle loop subsystems contain models for the optical and thermal efficiency of the solar field including receiver as well as for heat losses and parasitic power consumption calculations.

The optical efficiency is calculated for every hour of the year via a two-dimensional look-up table created in the heliostat field design tool HFLCAL [31]. The thermal efficiency of the CentRec® receivers is calculated from a simplified semi-analytical correlation with parameters derived from experiments and numerical models [32].

Heat losses from the TES, from particle transport and from PHX systems are estimated by use of constant thermal losses (in case of the TES) and constant thermal efficiencies. Similarly, power consumption of the vertical particle transport system is derived from the lifted mass and an estimated electric-to-mechanical efficiency. The chosen values for all parameters are given in Appendix A.

The thermal rating of a CSP plant's solar field compared with the design-point demand of the power block (known as the solar multiple), as well as the thermal energy storage capacity directly influence the capacity factor and achievable LCOE. As the optimal value of solar multiple and storage capacity depend on several factors, including costs, a parametric study is conducted for each assessed power cycle. The solar multiple is varied by changing the number of identical towers with associated heliostat fields (6 to 10 units) without re-optimization of the solar field. The storage capacity is defined in full load-equivalent hours and mainly influences the amount of dumped energy and the TES subsystem costs.

3.3. Economic models

The contributions to the plants' overall installation costs are calculated at two different levels of detail. The total cost of sCO₂ power blocks is calculated from component costs (provided by Siemens Energy) with cost adders for indirect costs. All other subsystems (heliostat fields, land, receivers, towers, transport system, PHX, TES and steam power block) are represented by more generic cost correlations derived from Heller et al. [24]. The numerical values, except those proprietary to Siemens Energy, are given in Appendices D and E.

It is noteworthy that all heat exchangers were priced on the basis of their surface area, A_{PHX} , as this is thought to be the most representative indicator. Due to the low technological maturity of particle-to-sCO₂ heat exchangers, cost correlations for them have a large uncertainty [24]. To demonstrate the sensitivity of optimal plant layout and overall LCOE on them, three different correlations were implemented and the results compared. Two of them are the lower bound (lb) and upper bound (ub) defined by Buck and Sment [33]:

$$C_{PHX,B\&S,lb} = 14.538 \text{ MUSD} + 4158 \text{ USD/m}^2 A_{PHX} \quad (2)$$

$$C_{PHX,B\&S,ub} = 14.538 \text{ MUSD} + 9031 \text{ USD/m}^2 A_{PHX}. \quad (3)$$

The third includes a TIT-dependent factor to account for less expensive materials in low-temperature PHXs:

$$C_{PHX,Carbo_02} = (1 + 2.1034 \times 10^{-2} (\Delta T_{ref}/K) + 1.24 \times 10^{-4} (\Delta T_{ref}/K)^2) \times 20\,293 \text{ USD} (A_{PHX}/\text{m}^2)^{0.66}, \quad (4)$$

wherein, $\Delta T_{ref} = \max(TIT - 550^\circ\text{C}, 0\text{K})$. The surface area of each PHX is calculated from its total conductance, UA , (which is an output of the thermodynamic model) and an estimated conductance, $U = 300 \text{ W}/(\text{m}^2\text{K})$. This latter value was chosen assuming a tubular moving bed heat exchanger, in which the overall heat transfer is dominated by the heat transfer on the particle side [24]. The effect of these three correlations on subsystem cost as well as the temperature-dependency of Eq. (4), are visualized in Fig. 4.

Furthermore, the adder for indirect costs (for electric equipment, instrumentation, civil works, etc.) and contingencies of the sCO₂ power blocks is estimated at a value of 67% of the equipment cost. While this

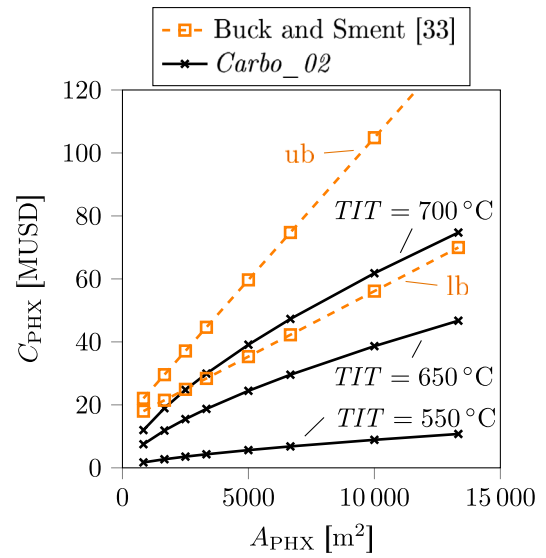


Fig. 4. Used PHX cost correlations [see Eqs. (2)–(4)]; ub: upper bound; lb: lower bound.

is higher than as anticipated in other studies, it is lower than that for the steam reference system [for more details see 21].

The LCOE is calculated through a simple approach: $LCOE = (FCR * C_{overnight} + C_{O\&M,a}) / E_{e,a}$. Therein, $C_{O\&M,a}$ represents the annual operation and maintenance costs (set to 2% of the direct costs of the EPC contractor), $C_{overnight}$ the project's overnight cost, $E_{e,a}$ the annual net electric output of the plant and FCR the fixed charge rate. Details on the method are described in the pre-study [21].

To make the results of this study more comparable with the extensive body of works surrounding the U.S. Gen3 Project [e.g. 23], the financing parameters were adjusted to equal those provided by the U.S. Department of Energy. This includes rather optimistic financing conditions of 5% annual interest rate and a depreciation period of 30 years, resulting in a fixed charge rate of 6.5%. The LCOE values of all configurations (including the reference system) are, hence, much lower than in previous studies [e.g. 21,24]. However, this does not significantly affect the comparison in this study and is in line with other Gen3 studies.

4. Results

In this section, calculated LCOE values are presented for the modeled particle CSP plants. The focus is on the comparison of techno-economic performance of plants featuring an sCO₂ power cycle with those relying on state-of-the-art steam technology. Further information is given on the optimum configurations in terms of solar field sizing, sCO₂ cycle and TIT selection as well as on comparative off-design performance.

4.1. LCOE comparison

The LCOE of all seven power block layouts over the solar multiple is depicted in Fig. 5. Each data point represents the configuration having the lowest LCOE considering all modeled TES capacities. Each of the three plots shows the results derived with one of the three PHX cost models. The main observations are the following:

- None of the sCO₂ configurations comes close to the reference system's LCOE. The difference in the respective optima is +9% to +13%.

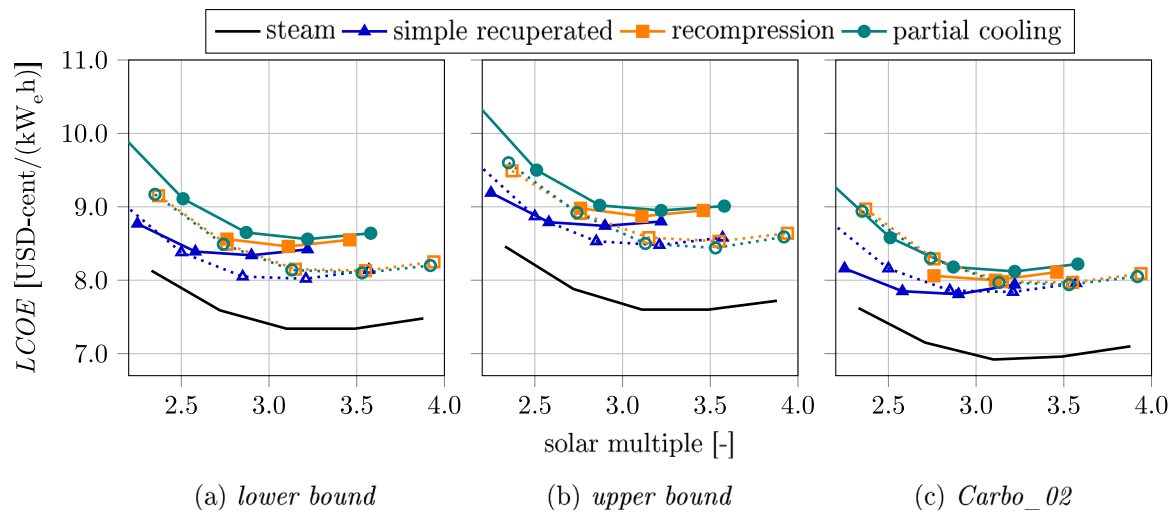


Fig. 5. LCOE values of all cycle variants calculated with the three PHX cost correlations (a)–(c); the TES capacity has been optimized for each data point (see Fig. 8); solid lines: $TIT = 550\text{ }^{\circ}\text{C}$; dashed lines: $TIT = 650\text{ }^{\circ}\text{C}$.

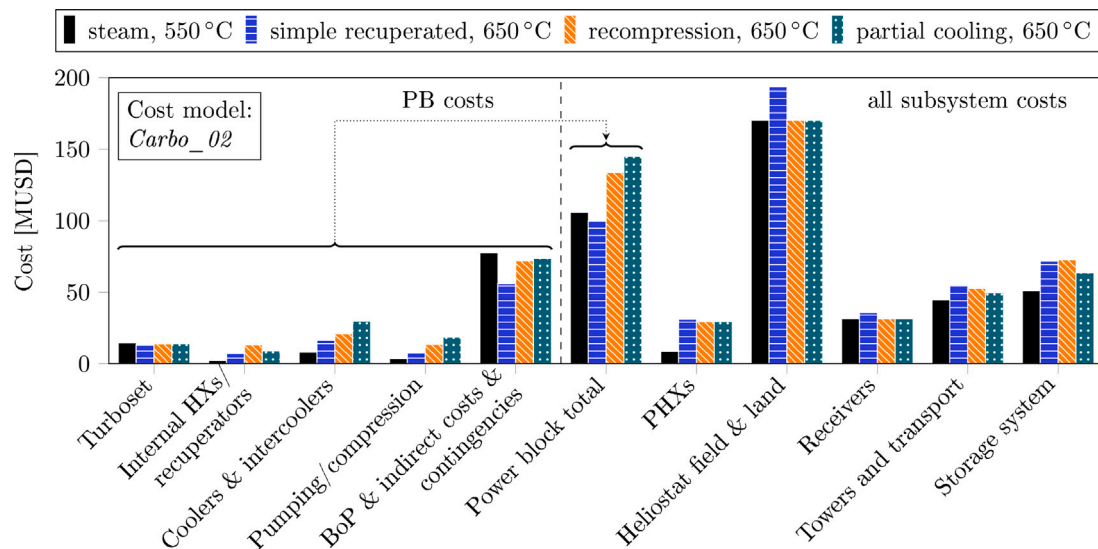


Fig. 6. Comparison of component and subsystem costs of three $s\text{CO}_2$ cycle plants and the reference steam plant, calculated with the developed cost model *Carbo_02*.

- Higher TITs (dashed lines) only improve the LCOE (by up to -5%) if the temperature impact on PHX costs is neglected (cost models *lower bound* and *upper bound*). A less steep temperature-dependent cost increase correlation might show slightly different results, though. When using Model *Carbo_02* (Eq. (4)), the LCOE is not significantly influenced by the TIT. In the preliminary study, a TIT of $550\text{ }^{\circ}\text{C}$ was found to be optimal in all cases. If the low solar multiple of that study is maintained (a value of approx. 2.4, see left bound of the plots), this holds true in most cases of the detailed simulation results as well.
- At a TIT of $550\text{ }^{\circ}\text{C}$, the lowest LCOE among the $s\text{CO}_2$ configurations is calculated for the simple recuperated cycle. At the higher TIT value, the economical performance of all three cycles is similar.
- The lowest LCOE values for all configurations are found for variants with a large SM (3.0... 3.6) and TES capacity ($14\text{ h}_{\text{FLE}} \dots 16\text{ h}_{\text{FLE}}$).
- The qualitative agreement between the results of the detailed model and those of the prestudy is good.

4.2. Comparison of component and subsystem costs

Fig. 6 depicts the component and subsystem costs for the reference system and for a variant of each $650\text{ }^{\circ}\text{C}$ $s\text{CO}_2$ process. To make the costs of the plants comparable, for each $s\text{CO}_2$ cycle a variant with similar electricity yield to the reference system was chosen ($< \pm 1\%$ difference) which also has one of the lowest LCOE values among the variants of that cycle. The PHX cost model *Carbo_02* was chosen because it considers changes in material costs depending on the component's design temperature.

It can be seen that the $s\text{CO}_2$ variants do not achieve significant cost savings in any category. The only exceptions are the indirect and BoP (balance of plant) costs of the simple recuperated cycle. It also has a slightly lower total power block cost than the reference system, but this is more than offset by the significantly higher costs of all solar subsystems due to the lower cycle efficiency.

The $s\text{CO}_2$ heat exchangers are decisive for the higher power plant unit costs. Recuperators, coolers and, in particular, the PHX (most pronounced in the *Carbo_02* cost model) are significantly more expensive than in the reference system. The reasons for this are larger amounts of transferred heat (in the case of recuperators) as well as higher fluid

pressures and temperatures. The sCO₂ compressors are also several times more expensive than the pumps of the steam system, which is mainly due to their greater number and higher rating.

The costs of the solar subsystems heliostat field, land, receiver and towers (excl. particle transport) are identical for all shown variants except for the simple recuperated plant. In the latter, the lower conversion efficiency necessitates a higher thermal input to achieve a similar electricity yield. Particle transport and TES subsystems are more expensive for sCO₂ variants, as the required throughput and inventory of particles are higher due to the smaller temperature spread.

The shown cost distributions of the optimal configurations are different to those in the preliminary study [21], although the power block component cost correlations are unchanged. This is mainly due to the significantly higher solar multiple values and also the updated correlations for PHX and solar system costs.

4.3. Off-design performance

Due to CSP plants' intermittent energy source and locations with commonly large changes in ambient temperature (paired with dry-cooling technology), their off-design performance can be of great significance. As no external load profile has been implemented in the presented models and the LCOE-optimized variants have large TES systems, part-load is much less prevalent, though. The thermal efficiency of the four variants compared in Section 4.2 for every hour of the year is depicted over ambient temperature in Fig. 7.

The three sCO₂ configurations perform qualitatively similar in off-design. Namely, they see a steep decline in thermal efficiency for ambient temperatures above the design point and only a marginal increase in efficiency for lower temperatures. The latter effect is only caused by lowered parasitic power consumption of the coolers and, hence, limited while the conditions in the cycle are kept mostly constant to avoid trans-critical behavior in the compressors (see Section 3.1.1). The steam cycle benefits more from a lower ambient temperature as the condensate pressure is lowered with it. This being said, the annual power block net efficiency for all cycles is close to its design point value.

The second difference between the sCO₂ configurations and the reference system is that each of the former produce a range of efficiency values for most ambient temperatures. These data points represent part-load behavior during start-up or final storage discharging. The effect of these lower efficiencies on the annual efficiency is, however, very small due to their rare occurrence.

4.4. Optima of storage capacity and PHX temperature difference

As described in Section 4.1, the TES capacity was varied to determine global LCOE minima. As expected, a higher value of the solar multiple also leads to a larger optimal storage capacity. Since the choice of PHX cost model has no major influence on this phenomenon, only the values calculated with the *Carbo_O2* model are depicted in Fig. 8. Systems with a TIT of 650 °C generally favor slightly larger storage capacities, as the additional costs of the TES are offset by higher annual utilization rates at higher power block costs. This effect outweighs the increase in specific storage costs due to higher cold tank temperatures with an increased TIT.

A reduction in the cold tank temperature can also be achieved by lowering the terminal temperature difference (TTD) of the PHX ($TTD = T_{hot\ side,out} - T_{cold\ side,in}$), from the so-far used value of 150 K. This also leads to a lower particle mass flow and particle inventory. The resulting cost advantages must be weighed against an increased PHX cost. In order to investigate this effect, the simulations described so far were carried out with TTD values between 50 K and 150 K.

When using either of the cost models *Carbo_O2* or *lower bound*, the optimum of all sCO₂ configurations lies at a PHX TTD of 50 K. Increasing the TTD to a value of 150 K leads to LCOE increases of up to

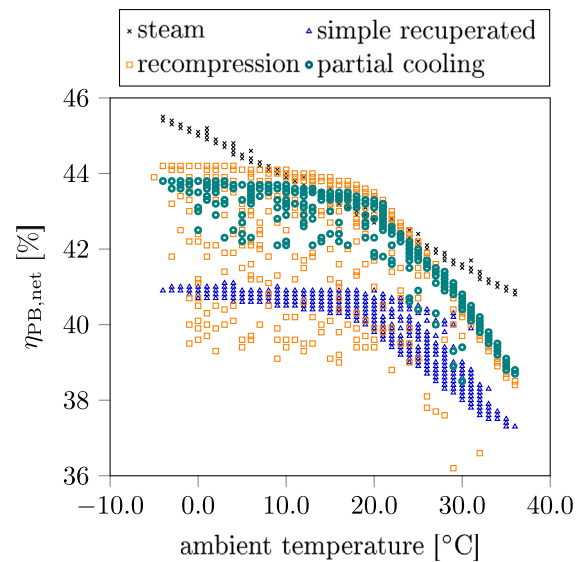


Fig. 7. Net power block efficiency in off-design conditions of four variants defined in Section 4.2; TIT = 650 °C; each data point represents one hour of the year.

4%. The particle steam generators have an optimum at TTD values of 25 K for the *Carbo_O2* cost model for all solar multiple variations (this value was implemented) and of 100 K for the *lower bound* model. Due to the lower costs of steam PHX, the influence on LCOE is smaller than that in sCO₂ systems.

For higher PHX costs (*upper bound* model), a change in the optimum TTD can be observed depending on the solar multiple (shown in Fig. 9). A higher value of the solar multiple leads to a higher utilization of the PHX and it is, therefore, worth investing in a PHX with a higher effectiveness.

To summarize, determining the TTD of the PHX has a noticeable influence on the LCOE of the overall system. However, the optimum depends heavily on the cost model used.

4.5. Component cost sensitivity analysis

Due to the rather large uncertainty in the cost models concerning yet-to-be-developed technology, a sensitivity analysis on the component costs was conducted. In that, the absolute cost of most power block components was multiplied by a factor with a value ranging from 0.5 to 1.5. For the component groups (i) recuperators, (ii) coolers and intercoolers,¹ (iii) turbines and compressors (excluding motors and generators) as well as (iv) indirect costs, no correlated changes in the costs of the reference steam cycle were assumed. Furthermore, the cost of the PHX subsystem was varied, however, the same changes were also applied to the (albeit much cheaper) steam PHX. Lastly, the costs of the reference cycle power block was varied.

For a clearer visualization of the effect of these sensitivities on the comparison of both technologies, the results are presented in Fig. 10 as the lowest LCOE of any sCO₂ configuration divided by that of any steam system. It is noteworthy that even in the most favorable — and almost certainly unrealistic — scenario shown, that is, all cost reductions of sCO₂ cycles are combined, they do not reach cost parity with the reference system irrespective of the PHX cost model employed. It needs to be pointed out, though, that such extreme changes in the cost models would most likely benefit cycle variations which were not modeled in this study, e.g. those with larger heat exchangers.

¹ The cost of coolers and intercoolers was only lowered down to a lower bound, defined by Siemens Energy, representing a fraction of approximately 0.8.

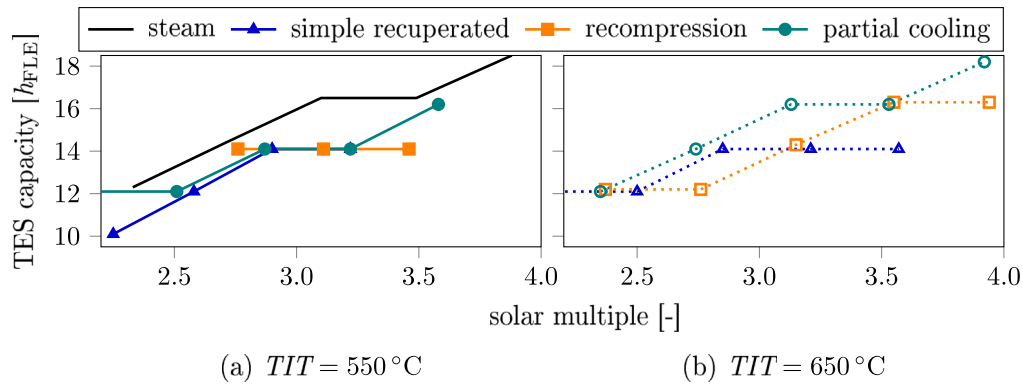


Fig. 8. Optimum TES capacity over solar multiple when using the *Carbo_02* PHX cost model.

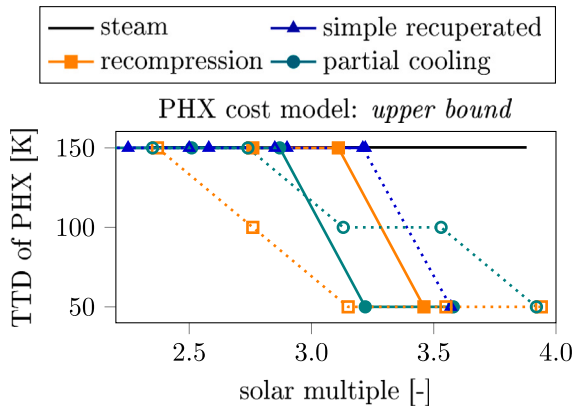


Fig. 9. Optimum TTD of PHX when using the *upper bound* cost model; solid lines: TIT = 550°C; dashed lines: TIT = 650°C.

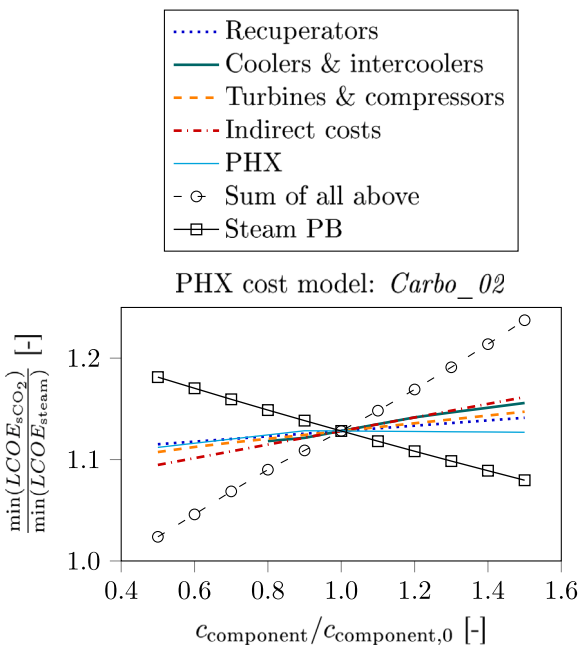


Fig. 10. Sensitivity analysis for ratio of sCO₂ over steam cycle LCOE depending on variations in component and subsystem costs.

Table 3

Changed parameters between simplified selection models in the pre-study [21] and in this study; dp: design point; a: annual; †: changed because of an error in the pre-study.

Parameter	Unit	Pre-study	This study
Annual interest rate	[% p.a.]	8	5
Plant lifetime	[a]	25	30
Solar multiple	[-]	2.5	3.5
Storage capacity	[h _{FLE}]	12	16
<i>Efficiencies</i>			
Heliostat field, dp	[%]	73.5	64.9
Heliostat field, a	[%]	52.7	55.4
Receiver, a	[%]	86.7	87.0
Thermal efficiency of particle transport	[%]	100	98
Plant gross-to-net	[%]	97.5	98.7
$\eta_{PB,net,a}/\eta_{PB,net,dp}$	[%]	99.0	98.0
Steam 550°C: $\eta_{PB,net,dp}^\dagger$	[%]	42.7	43.7
Steam 600°C: $\eta_{PB,net,dp}^\dagger$	[%]	43.9	44.7

4.6. Rerun of pre-study

The six sCO₂ configurations which were investigated in this study had been selected in a simplified techno-economic simulation [21]. That pre-selection neither included hourly off-design simulations of the solar field or the power block, nor an optimization of the solar multiple or TES capacity. Furthermore, several cost correlations and financial parameters have been refined during the detailed modeling of the cycles. Hence, it is possible that certain processes and parameters were discarded in the pre-selection which would have provided better results than the chosen configurations once modeled in detail. To confirm the original pre-selection, it was repeated with updated assumptions. The absolute values of the LCOE between the two simulation runs are not comparable, but the relative comparison between the configurations is valid.

The differences between the pre-selection in Ref. [21] and the rerun concern the following parameters (quantitative values are given in Table 3):

- Cost models for land, receivers, transport systems, towers and TES system as well as currency conversion rate (compare Appendix E with Ref. [21, Table A5]);
- Financial parameters: annual interest rate and depreciation period; These changes, made in order to improve comparability with other studies (see Section 3.3), have a large influence on the overall LCOE of all configurations.
- Solar multiple and TES capacity; As shown in Fig. 5, this has a significant influence on the economic ranking of variants.
- Changes in design-point and annual efficiencies of several subsystems; This affects all cycles.

The Pareto fronts of the LCOE values for each cycle as calculated with the original and with the updated preselection model are shown

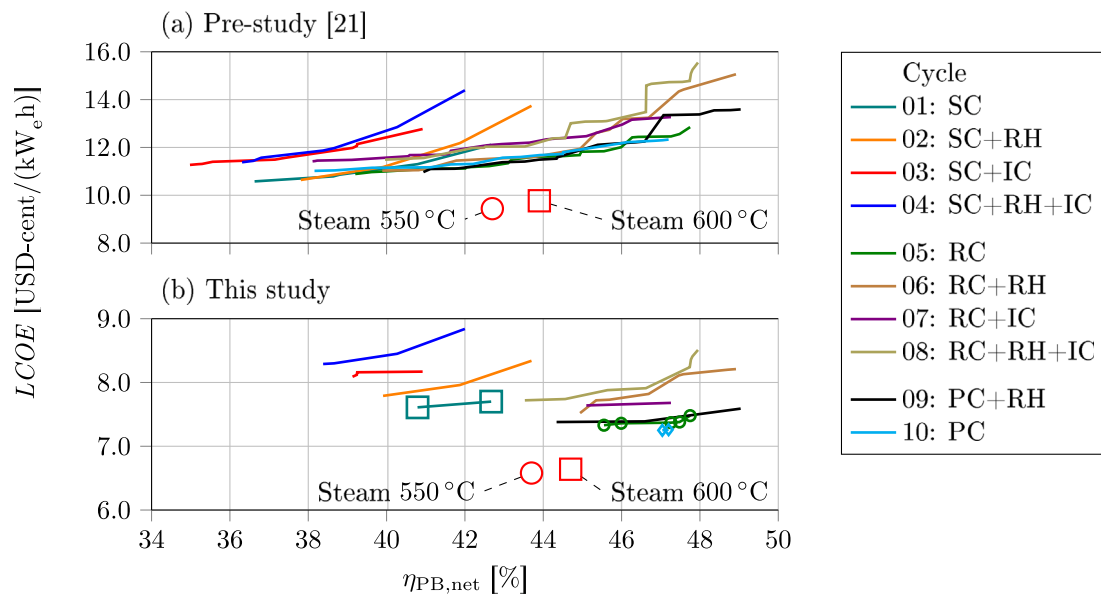


Fig. 11. Pareto fronts of the LCOE values for each cycle as calculated in the (a) pre-selection and (b) repeated selection; SC: simple recuperated cycle; RH: reheat; IC: intercooling; RC: recompression cycle; PC: partial cooling cycle (for details, see [21]).

in Fig. 11(a) and (b), respectively. According to the updated model, configurations with significantly higher efficiencies are favored. However, the implementation of reheating or intercooling is still not found to be economical. The selection of the basic configurations of the simple recuperated, recompression and partial cooling cycles (Cycles 01, 05 and 10) is therefore still justified. The differences between TITs at different levels continue to be reflected primarily in the efficiency, but not in the LCOE values (not shown). As two TIT values were modeled in the detailed annual calculations, no correction to the selected value of this parameter is needed either.

Finally, it must be investigated whether changes to the remaining process parameters (heat exchanger ratings, turbine outlet pressure, intermediate pressures and recompression fractions) would have led to fundamentally different findings. For this purpose, the optimum values of these parameters were identified for the six selected variants (Types 01, 05 and 10 with TITs of 550 °C and 650 °C, respectively) using the updated preselection models and their LCOE was calculated. Furthermore, the LCOE values of the originally chosen variants for these six cycles were also calculated with the updated model. The following observations were made when comparing the LCOE values of the two variants of each cycle:

- For the simple recuperated process, there is no change in the optimal parameters for either TIT value.
- For the recompression cycle at a TIT of 550 °C, there is a difference in the optimum LCOE value of less than 0.4% due to the modified modeling. By additionally using the significantly higher values for solar multiple and TES capacity, this difference increases to up to 2.8%.
- For the recompression cycle at a TIT of 650 °C, the changes are less than 0.5% and 1.9%, respectively.
- For the partial cooling processes, the change is less than 1.4% and 0%, respectively.

It can, therefore, be concluded that the cycles which would have been selected using the updated version of the preselection model do not differ significantly from those which had previously been chosen for the detailed assessments.

5. Conclusions

In this study, the potential cost benefit of using pure sCO₂ cycles in next-generation CSP plants was assessed. Techno-economic models

of seven power plants based on high-temperature particle receivers in a multi-tower configuration were created: Six of them featuring variants of sCO₂ cycles and, to enable a fair comparison of technologies, one reference system using a commercially available state-of-the-art steam cycle. The results of hourly yield simulations and detailed cost calculations indicate that the lowest LCOE of any sCO₂ process is at least 9% higher than that of the reference system. Compared with this difference, the impact of selecting one of the three modeled sCO₂ cycles or one of the two temperature levels is small. Due to the large uncertainty of costs for the particle heat exchanger, three different cost models for this component were implemented. However, this does not have a decisive effect on the comparison to the reference system either. A sensitivity analysis on the LCOE comparison showed that even at cost reductions of 50% for most sCO₂ cycle components, no cost benefit would be achieved.

Cause for these unfavorable results for sCO₂ systems are mainly higher component costs of all involved heat exchangers (PHXs, recuperators and coolers) as well as of compressors and motors. High-efficiency cycles are further penalized because they generally have lower temperature spreads between hot and cold storage tanks, leading to an increase in costs of the TES and particle transport subsystems. While the off-design performance of the sCO₂ cycles is qualitatively different to that of the reference system, its influence on the plants' annual yield is small.

The results of this study indicate that future research and development on next-generation utility-scale CSP plants should not be limited to those utilizing sCO₂ power cycles but instead consider the specific advantages and specifications of currently available or even advanced steam cycles. While it is possible that technological and manufacturing breakthroughs lead to lower costs of sCO₂-specific components (e.g., compact heat exchangers) or higher efficiencies (e.g., through the use of sCO₂ blends), it is by no means guaranteed that this will lead to an economic advantage over the state of the art. In other applications, out of the scope of the present study, sCO₂ can, however, be cost-competitive (e.g. smaller systems, those operating at medium temperatures, combined processes or so-called Carnot batteries).

CRedit authorship contribution statement

Lukas Heller: Writing – original draft, Visualization, Software, Methodology, Investigation, Formal analysis, Conceptualization. **Stefan**

Glos: Writing – review & editing, Validation, Methodology, Investigation. **Reiner Buck:** Writing – review & editing, Software, Methodology, Funding acquisition, Conceptualization.

Declaration of competing interest

The authors declare that they have no known competing financial interests or personal relationships that could have appeared to influence the work reported in this paper.

Acknowledgments

The authors would like to thank the German Federal Ministry for Economic Affairs and Climate Action for the financial support of the project CARBOSOLA (reference number: 03EE5001). Furthermore, thanks are due to several reviewers for their valuable input.

Appendix A. Data book

See Table A.1.

Appendix B. *T-s* (temperature–entropy) diagrams of sCO₂ cycles

See Fig. B.1.

Appendix C. State points of sCO₂ cycles with a TIT of 650 °C

See Table C.1.

Appendix D. Cost models of power block components and subsystems

See Table D.1.

Table A.1
Input parameters for thermodynamic models.

Parameter	Unit	Value	Comments/Source
<i>Location</i>			
Name	[]	Postmasburg, ZA	
Latitude	[°]N	−28.2980	
Longitude	[°]E	23.366	
Elevation	[m]	1514	Meteonorm 6.1
Ambient temp. (min./max./mean)	[°C]	−5.1/35.7/17.0	Meteonorm 6.1
Ambient pressure (min./max./mean)	[mbar]	841/861/852	Meteonorm 6.1
Annual direct normal irradiance	[kWh/(m ² a)]	2676	Meteonorm 6.1
<i>Design point</i>			
Design point	[DD.MM. hh:mm]	21.09. 12:00	
Direct normal irradiance, DNI	[W/m ²]	992 (clear sky)	For Design of plant in HFLCAL, clear-sky model is used [31] to calculate the DNI as a function of location, date and time.
Ambient temp.	[°C]	19.0	Same as power block
Amb. pressure	[mbar]	850	
Atmospheric attenuation: clear	[]	$0.99321 - 1.176 \times 10^{-4} \times SLR + 1.97 \times 10^{-8} \times SLR^2$ @ $SLR \leq 1000$ m; $e^{-1.106 \times 10^{-4} \times SLR}$ @ $SLR > 1000$ m	Needed for solar field design in HFLCAL; standard model [34]; <i>SLR</i> : slant range
<i>Heliostats</i>			
Heliostat type	[]	two-axis, multi facet	Based on Sanlucar 120
Aperture width	[m]	12.84	
Aperture height	[m]	9.45	
Mirrors per heliostat	[−]	28 (4 × 7)	horizontal x vertical
Reflecting area per mirror	[m ²]	4.33	
Optical height (pylon)	[m]	5.02	heliostat center
Reflecting area per heliostat	[m ²]	121	
Reflectivity HFLCAL (annual mean)	[%]	89.34	HFLCAL Input; product of reflectivity (0.94), cleanliness (0.96), availability (0.99)
Beam quality	[mrad]	3.25	HFLCAL Input; combination of slope, tracking and sun shape error
Canting	[]	on-axis	
Power consumption tracking	[kW _e]	0	Neglected in annual yield calculation
<i>Solar field</i>			
Number of towers	[−]	varied	
Orientation	[]	South	
Tower height above center of receiver	[m]	17	Estimate; needed for shading

(continued on next page)

Table A.1 (continued).

Parameter	Unit	Value	Comments/Source
<i>Receiver</i>			
Type	[]	cylindrical cavity	
Thermal rating	[MW _t]	96.23	Estimate for commercial system
HTM inlet temp.	[°C]	468	Estimate
HTM outlet temp.	[°C]	905	
Receiver model	[]	103	HFLCAL models
Absorption	[-]	0.95	Parameter for receiver models
Emissivity	[-]	0.90	Buck and Giuliano [35]
Convection heat transfer coeff.	[W/(m ² K)]	30	
Reference temp.	[°C]	905	
Min./max. load	[%]	10/115	Estimate
Particle loss rate	[%/a]	0	Neglected
Elec. consumption	[kW _e]	0	Neglected
Start up time	[min]	20	Giuliano et al. [34, p. 479]
Heat demand start-up (per tower)	[kW _t h]	891	Estimate
Power demand start-up	[kW _e h]	0	Neglected
<i>HTM</i>			
Name	[]	Bauxite	
Heat capacity	[J/(kg K)]	1200	Siegel et al. [36]
Bulk density	[kg/m ³]	2000	Siegel et al. [36]
<i>Vertical HTM transport</i>			
Transport height tower	[m]	139	incl. top installations
Transport height PHX	[m]	30	Estimate
Efficiency vert. transport system	[%]	75	Estimate
<i>Horizontal HTM transport</i>			
Energy consumption	[MW _e]	0	Neglected
Thermal losses	[%]	2	of transp. energy
<i>TES system</i>			
Hot tank temp.	[°C]	900	
Cold tank temp.	[°C]	400	
Heat loss	[%/24 h]	1	of total capacity
<i>PHX</i>			
Pressure drop, steam	[%]	1	Estimate
Heat loss	[%]	0	Neglected

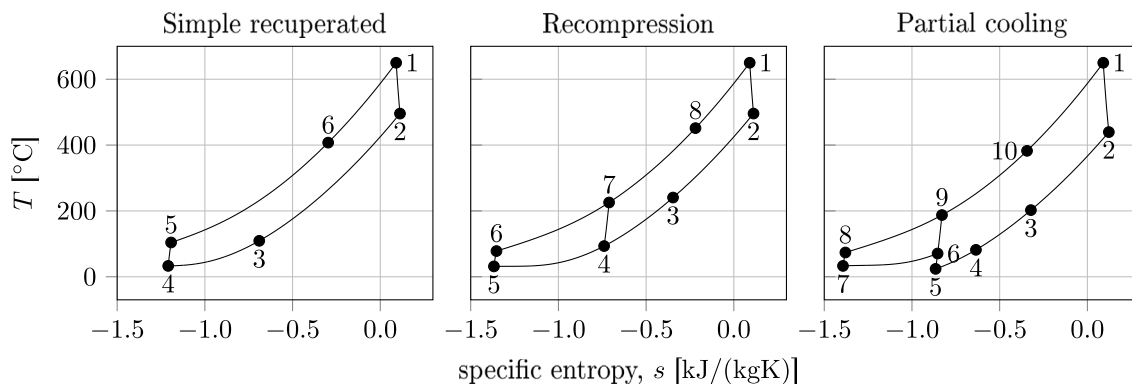


Fig. B.1. Temperature–entropy ($T-s$) diagram of investigated $s\text{CO}_2$ cycles with a TIT of 650°C .

Table C.1
State points of modeled sCO₂ cycles (numbering according to Fig. B.1).

	Simple recuperated			Recompression			Partial cooling		
	<i>T</i> [°C]	<i>p</i> [bar _a]	<i>h</i> [kJ/(kg K)]	<i>T</i> [°C]	<i>p</i> [bar _a]	<i>h</i> [kJ/(kg K)]	<i>T</i> [°C]	<i>p</i> [bar _a]	<i>h</i> [kJ/(kg K)]
1	650.0	260.0	650.8	650.0	260.0	650.8	650.0	260.0	650.8
2	495.6	78.5	473.0	495.7	78.6	473.1	439.4	47.8	410.9
3	109.2	76.9	27.3	240.7	77.0	179.8	202.5	46.9	147.6
4	33.0	76.4	-144.5	93.3	75.5	7.7	81.8	45.9	17.1
5	104.2	273.5	-100.3	31.5	75.0	-193.2	24.0	45.7	-57.6
6	407.5	265.3	345.4	78.1	282.0	-157.5	70.6	80.0	-29.8
7				225.7	273.5	107.2	33.0	79.7	-200.2
8				451.5	265.3	400.5	73.7	282.0	-166.7
9							187.5	273.5	50.7
10							382.5	265.3	314.1

Table D.1
Cost models of power block (*: confidential data; if no source is mentioned, the correlation was created within the CARBOSOLA Project; assumed exchange rate: 1 EUR = 1.185 USD; TP: technology provider; \dot{V}_{in} : volumetric flow rate at inlet; †: Buck and Giuliano [32]; §: Weiland et al. [37]; ‡: Heller et al. [24]).

Component/subsystem	<i>x</i>	$C = (1 + d \times T_{reference} + e \times T_{reference}^2)(a + bx^c)$					Source
		Coefficients					
		<i>a</i> [USD]	<i>b</i> [USD]	<i>c</i>	<i>d</i>	<i>e</i>	
PHXs	$UA/(W_t/K)$	see Eq. (2)...(4)					
Recuperators	$UA/(W_r/K)$	*	*	*	*	-	
Coolers	$UA/(W_c/K)$	*	*	*	-	-	
Intercoolers	$UA/(W_i/K)$	*	*	*	-	-	
Turbines	P_m/W_m	*	*	*	*	-	
Compressors	$\dot{V}_{in}/(m^3/s)$	*	*	*	-	-	
Motors	P_e/W_e	-	399 400	0.6062	-	§	
Generator	P_e/W_e	-	108 900	0.5463	-	§	
Additional piping and valves	sum of costs above	-	5%	1	-	-	
Piping high-pressure	$\dot{V}_{in}/(m^3/s)$	-	*	*	*	-	
Piping low-pressure	$\dot{V}_{in}/(m^3/s)$	-	*	*	*	-	
Additional sCO ₂ BoP	-	2×10^6	-	-	-	-	
Indirect PB cost incl. TP profit	$C_{PB,equipment}$	-	67%	1	-	-	
Steam reference cycle	$P_{e,net}/W_e$	-	*	1	-	-	
Indirect steam PB cost incl. TP profit	$C_{PB,equipment}$	-	83%	1	-	-	

Table E.1
Cost models of solar subsystems (assumed exchange rate: 1 EUR = 1.185 USD; $H_{tower,opt}$: height of receiver center above tower base; ρ_{land} : land usage factor, estimated at 20%; †: Buck and Giuliano [32]; §: Weiland et al. [37]; ‡: Heller et al. [24]; §: Albrecht et al. [38]).

Subsystem	Cost correlation	Source
Heliostat field	$118.5 \text{ USD}/m^2 \times A_{heliostats}$	†
Land	$2.37 \text{ USD}/m^2 \times A_{heliostats}/\rho_{land}$	† ‡
Receiver	$94 800 \text{ USD}/m^2 \times A_{Rec,apert}$	DLR estimate
1 Tower incl. TES integration	$(1.759 \text{ MUSD} + 257 \text{ USD}(H_{tower,opt}/m)^{1.94} + 516 \text{ USD}(H_{tower,opt}/m)^{1.81})/2$	‡
Vertical transport system	$58.37 \text{ USD}/(m \text{ kg}/s) \times H_{transport} \times \dot{m}_{Pa,dp}$	$H_{transport} = 30 \text{ m}$ for PHX; $H_{transport} = H_{tower,opt} + 10 \text{ m}$ for towers §
Horizontal transport system	$126 582 \text{ USD} \times n_{vehicles} + 42 194 \text{ USD} \times n_{towers}$	‡
Particle inventory	$1.185 \text{ USD}/\text{kg} \times m_{particles}$	‡
TES system (excl. inventory)	see Heller et al. [24, Appendix A.1]	

Appendix E. Cost models of solar subsystems

See Table E.1.

References

[1] Y. Ahn, S.J. Bae, M. Kim, S.K. Cho, S. Baik, J.I. Lee, J.E. Cha, Review of supercritical CO₂ power cycle technology and current status of research and development, Nucl. Eng. Technol. 47 (6) (2015) 647–661, <http://dx.doi.org/10.1016/j.net.2015.06.009>.

[2] T. Neises, C. Turchi, A comparison of supercritical carbon dioxide power cycle configurations with an emphasis on CSP applications, Energy Procedia 49 (2014) 1187–1196, <http://dx.doi.org/10.1016/j.egypro.2014.03.128>.

[3] Office of Energy Efficiency & Renewable Energy, Generation 3 concentrating solar power systems (Gen3 CSP) phase 3 project selection, 2022, URL <https://www.energy.gov/eere/solar/generation-3-concentrating-solar-power-systems-gen3-csp-phase-3-project-selection>.

[4] J. Dersch, J.I. Labairu, L. Schomaker, M. Schlecht, L. Pfundmaier, F. Zimmermann, PV-CSP hybrid power plants: Cost savings by close coupling and least cost design, AIP Conf. Proc. 2815 (1) (2023) 030005, <http://dx.doi.org/10.1063/5.0148693>.

[5] J.-M. Yin, Q.-Y. Zheng, Z.-R. Peng, X.-R. Zhang, Review of supercritical CO₂ power cycles integrated with CSP, Int. J. Energy Res. 44 (3) (2019) 1337–1369, <http://dx.doi.org/10.1002/er.4909>.

[6] J. Dyreby, S. Klein, G. Nellis, D. Reindl, Design considerations for supercritical carbon dioxide brayton cycles with recompression, J. Eng. Gas Turbines Power 136 (10) (2014) <http://dx.doi.org/10.1115/1.4027936>.

[7] C.S. Turchi, M. Boyd, D. Kesseli, P. Kurup, M.S. Mehos, T.W. Neises, P. Sharan, M.J. Wagner, T. Wendelin, CSP systems analysis - final project report, (NREL/TP-5500-72856) 2019, <http://dx.doi.org/10.2172/1513197>.

[8] R.P. Merchán, L.F. González-Portillo, J. Muñoz-Antón, Techno-economic analysis of the optimum configuration for supercritical carbon dioxide cycles in concentrating solar power systems, Entropy 26 (2) (2024) <http://dx.doi.org/10.3390/e26020124>.

[9] C.K. Ho, M. Carlson, P. Garg, P. Kumar, Technoeconomic analysis of alternative solarized s-CO₂ brayton cycle configurations, J. Sol. Energy Eng. 138 (5) (2016) <http://dx.doi.org/10.1115/1.4033573>.

- [10] V.T. Cheang, R.A. Hedderwick, C. McGregor, Benchmarking supercritical carbon dioxide cycles against steam rankine cycles for concentrated solar power, *Sol. Energy* 113 (2015) 199–211, <http://dx.doi.org/10.1016/j.solener.2014.12.016>.
- [11] F. Crespi, D. Sánchez, T. Sánchez, G.S. Martínez, Capital cost assessment of concentrated solar power plants based on supercritical carbon dioxide power cycles, *J. Eng. Gas Turbines Power* 141 (7) (2019) <http://dx.doi.org/10.1115/1.4042304>.
- [12] F. Crespi, D. Sánchez, G.S. Martínez, T. Sánchez-Lencero, F. Jiménez-Espadafor, Potential of supercritical carbon dioxide power cycles to reduce the levelised cost of electricity of contemporary concentrated solar power plants, *Appl. Sci.* 10 (15) (2020) 5049, <http://dx.doi.org/10.3390/app10155049>.
- [13] T. Neises, C. Turchi, Supercritical carbon dioxide power cycle design and configuration optimization to minimize levelized cost of energy of molten salt power towers operating at 650 °C, *Sol. Energy* 181 (2019) 27–36, <http://dx.doi.org/10.1016/j.solener.2019.01.078>.
- [14] S. Guccione, R. Guedez, Techno-economic optimization of molten salt based CSP plants through integration of supercritical CO₂ cycles and hybridization with PV and electric heaters, *Energy* 283 (2023) 128528, <http://dx.doi.org/10.1016/j.energy.2023.128528>.
- [15] R. Chen, M. Romero, J. González-Aguilar, F. Rovense, Z. Rao, S. Liao, Design and off-design performance comparison of supercritical carbon dioxide Brayton cycles for particle-based high temperature concentrating solar power plants, *Energy Convers. Manag.* 232 (2021) 113870, <http://dx.doi.org/10.1016/j.enconman.2021.113870>.
- [16] G. Manzolini, M. Binotti, E. Morosini, D. Sanchez, F. Crespi, G. Di Marcoberdino, P. Iora, C. Invernizzi, Adoption of CO₂ blended with C6f6 as working fluid in CSP plants, *AIP Conf. Proc.* 2445 (1) (2022) 090005, <http://dx.doi.org/10.1063/5.0086520>.
- [17] P. Rodríguez-deArriba, F. Crespi, S. Pace, D. Sánchez, Mapping the techno-economic potential of next-generation CSP plants running on transcritical CO₂-based power cycles, *Energy* 310 (2024) 133142, <http://dx.doi.org/10.1016/j.energy.2024.133142>.
- [18] E. Morosini, E. Villa, G. Quadrio, M. Binotti, G. Manzolini, Solar tower CSP plants with transcritical cycles based on CO₂ mixtures: A sensitivity on storage and power block layouts, *Sol. Energy* 262 (2023) 111777, <http://dx.doi.org/10.1016/j.solener.2023.05.054>.
- [19] F. Crespi, P. Rodríguez-deArriba, D. Sánchez, L. García-Rodríguez, Principles of operational optimization of CSP plants based on carbon dioxide mixtures, *Appl. Therm. Eng.* 260 (2025) 124871, <http://dx.doi.org/10.1016/j.applthermaleng.2024.124871>.
- [20] L. Heller, S. Glos, R. Buck, sCO₂ power cycle design without heat source limitations: Solar thermal particle technology in the CARBOSOLA project, in: 4th European sCO₂ Conference for Energy Systems: March 23–24, 2021, in: Online Conference, 2021, pp. 177–184, <http://dx.doi.org/10.17185/duublico/73961>, URL https://duublico2.uni-due.de/receive/duublico_mods_00073961.
- [21] L. Heller, S. Glos, R. Buck, Techno-economic selection and initial evaluation of supercritical CO₂ cycles for particle technology-based concentrating solar power plants, *Renew. Energy* 181 (2022) 833–842, <http://dx.doi.org/10.1016/j.renene.2021.09.007>.
- [22] M.R. Rodríguez-Sánchez, A. Sánchez-González, P.A. González-Gómez, C. Marugán-Cruz, D. Santana, Thermodynamic and economic assessment of a new generation of subcritical and supercritical solar power towers, *Energy* 118 (2017) 534–544, <http://dx.doi.org/10.1016/j.energy.2016.10.079>.
- [23] R. Buck, G3P3 techno-economic analysis of Up-Scaled CentRec[®] receiver, 2021, URL <https://elib.dlr.de/140177/>.
- [24] L. Heller, D. Többen, T. Hirsch, R. Buck, The cost-saving potential of next-generation particle technology CSP with steam cycles, *Sol. Energy* 263 (2023) 111954, <http://dx.doi.org/10.1016/j.solener.2023.111954>.
- [25] W. Wu, L. Amsbeck, R. Buck, R. Uhlig, R. Ritz-Paal, Proof of concept test of a centrifugal particle receiver, *Energy Procedia* 49 (2014) 560–568, <http://dx.doi.org/10.1016/j.egypro.2014.03.060>.
- [26] M. Ebert, L. Amsbeck, J. Rheinländer, B. Schlögl-Knothe, S. Schmitz, M. Sibum, R. Uhlig, R. Buck, Operational experience of a centrifugal particle receiver prototype, *AIP Conf. Proc.* 2126 (1) (2019) 030018, <http://dx.doi.org/10.1063/1.5117530>.
- [27] D. Alfani, M. Astolfi, M. Binotti, P. Silva, Effect of the ambient temperature on the performance of small size sCO₂ based pulverized coal power plants, in: 4th European sCO₂ Conference for Energy Systems: March 23–24, 2021, in: Online Conference, 2021, pp. 379–388, <http://dx.doi.org/10.17185/duublico/73981>, URL https://duublico2.uni-due.de/receive/duublico_mods_00073981.
- [28] T. Neises, Steady-state off-design modeling of the supercritical carbon dioxide recompression cycle for concentrating solar power applications with two-tank sensible-heat storage, *Sol. Energy* 212 (2020) 19–33, <http://dx.doi.org/10.1016/j.solener.2020.10.041>.
- [29] E. Liese, J. Albright, S.A. Zitney, Startup, shutdown, and load-following simulations of a 10 MWe supercritical CO₂ recompression closed Brayton cycle, *Appl. Energy* 277 (2020) 115628, <http://dx.doi.org/10.1016/j.apenergy.2020.115628>.
- [30] M.T. Luu, D. Milani, R. McNaughton, A. Abbas, Dynamic modelling and start-up operation of a solar-assisted recompression supercritical CO₂ brayton power cycle, *Appl. Energy* 199 (2017) 247–263, <http://dx.doi.org/10.1016/j.apenergy.2017.04.073>.
- [31] P. Schwarzboezl, R. Pitz-Paal, M. Schmitz, Visual HFLCAL - a software tool for layout and optimisation of heliostat fields, in: SolarPACES 2009, 2009, URL <https://elib.dlr.de/60308/>.
- [32] R. Buck, S. Giuliano, Impact of solar tower design parameters on sCO₂-based solar tower plants, in: 2nd European sCO₂ Conference 2018, 2018, <http://dx.doi.org/10.17185/duublico/46098>.
- [33] R. Buck, J. Sment, Techno-economic analysis of multi-tower solar particle power plants, *Sol. Energy* 254 (2023) 112–122, <http://dx.doi.org/10.1016/j.solener.2023.02.045>.
- [34] S. Giuliano, M. Puppe, H. Schenk, T. Hirsch, M. Moser, T. Fichter, J. Kern, F. Trieb, M. Engelhard, S. Hurler, A. Weigand, D. Brakemeier, J. Kretschmann, U. Haller, R. Klingler, C. Breyer, S. Afanasyeva, THERMVOLT: Systemvergleich von solarthermischen und photovoltaischen kraftwerken für die versorgungssicherheit, 2016, <http://dx.doi.org/10.2314/GBV:100051305X>.
- [35] R. Buck, S. Giuliano, Solar tower system temperature range optimization for reduced LCOE, *AIP Conf. Proc.* 2126 (1) (2019) 030010, <http://dx.doi.org/10.1063/1.5117522>.
- [36] N.P. Siegel, M.D. Gross, R. Coury, The development of direct absorption and storage media for falling particle solar central receivers, *J. Sol. Energy Eng.* 137 (4) (2015) <http://dx.doi.org/10.1115/1.4030069>.
- [37] N.T. Weiland, B.W. Lance, S.R. Pidaparti, sCO₂ power cycle component cost correlations from DOE data spanning multiple scales and applications, in: Proceedings of ASME Turbo Expo 2019: Turbomachinery Technical Conference and Exposition GT2019 Volume 9: Oil and Gas Applications; Supercritical CO₂ Power Cycles; Wind Energy, 2019, <http://dx.doi.org/10.1115/gt2019-90493>.
- [38] K.J. Albrecht, M.L. Bauer, C.K. Ho, Parametric analysis of particle CSP system performance and cost to intrinsic particle properties and operating conditions, 2019, <http://dx.doi.org/10.1115/es2019-3893>,